Proc. Natl. Acad. Sci. USA
Vol. 93, pp. 10078–10083, September 1996
Biochemistry

Ultrasensitivity in the mitogen-activated protein kinase cascade

CHI-YING F. HUANG AND JAMES E. FERRELL, JR.†

Department of Molecular Pharmacology, Stanford University School of Medicine, Stanford, CA 94305-5332

Communicated by Daniel E. Koshland, Jr., University of California, Berkeley, CA, May 16, 1996 (received for review January 22, 1996)

ABSTRACT **The mitogen-activated protein kinase (MAPK) cascade is a highly conserved series of three protein kinases implicated in diverse biological processes. Here we demonstrate that the cascade arrangement has unexpected consequences for the dynamics of MAPK signaling. We solved the rate equations for the cascade numerically and found that MAPK is predicted to behave like a highly cooperative enzyme, even though it was not assumed that any of the enzymes in the cascade were regulated cooperatively. Measurements of MAPK activation in *Xenopus* oocyte extracts confirmed this prediction. The stimulus/response curve of the MAPK was found to be as steep as that of a cooperative enzyme with a Hill coefficient of 4–5, well in excess of that of the classical allosteric protein hemoglobin. The shape of the MAPK stimulus/response curve may make the cascade particularly appropriate for mediating processes like mitogenesis, cell fate induction, and oocyte maturation, where a cell switches from one discrete state to another.**

Although the biological responses associated with mitogen-activated protein kinase (MAPK) signaling are highly varied, the basic structure of the MAPK cascade is well conserved (1–3). The cascade always consists of a MAPK kinase kinase (MAPKKK), a MAPK kinase (MAPKK), and a MAPK. MAPKKKs activate MAPKKs by phosphorylation at two conserved serine residues and MAPKKs activate MAPKs by phosphorylation at conserved threonine and tyrosine residues (Fig. 1). The cascade relays signals from the plasma membrane to targets in the cytoplasm and nucleus.

A number of other membrane-to-nucleus signaling pathways, such as the Jak/Stat pathways and the cAMP/protein kinase A pathway, employ just a single protein kinase. Why does the MAPK cascade invariably use three kinases instead of one? The possibility that the three kinase arrangement has evolved to allow signal ramification or amplification is attractive but, as yet, not well supported by genetic or biochemical evidence.

We have explored the possibility that the cascade arrangement has important consequences for the dynamics of MAPK signaling. Here we shall focus on the steady-state responses of enzymes at each level in the cascade to varying input stimuli. The stimulus/response curve of a typical Michaelis–Menten enzyme is hyperbolic, and the enzyme responds in a graded fashion to increasing stimuli. An 81-fold increase in stimulus is needed to drive the enzyme from 10% to 90% maximal response (see for example, the MAPKKK curves in Fig. 2). However, some enzymes exhibit stimulus/response curves that are steeper or less steep than the Michaelis–Menten curve. Goldbeter and Koshland have termed these responses "ultrasensitivity" and "subsensitivity," respectively (11–13). An ultrasensitive enzyme requires less than an 81-fold increase in stimulus to drive it from 10% to 90% maximal response (for example, the MAPK and MAPKK curves in Fig. 2); a subsensitive enzyme requires more than an 81-fold increase.

The term ultrasensitivity emphasizes the fact that the upstroke of the stimulus/response curve is steeper than that of a hyperbolic Michaelis–Menten enzyme, as shown in Fig. 2*A*. However,

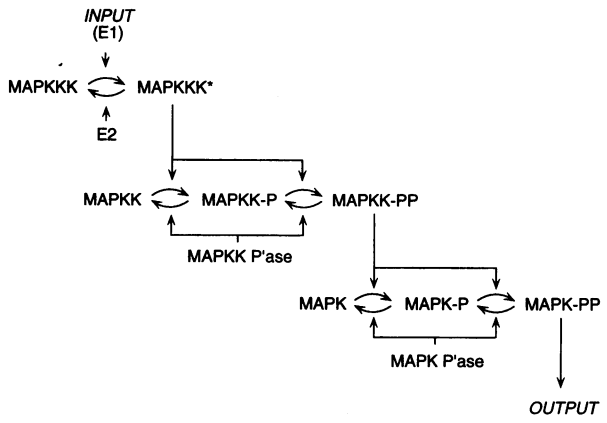

FIG. 1. Schematic view of the MAPK cascade. Activation of MAPK depends upon the phosphorylation of two conserved sites [Thr-183 and Tyr-185 in rat p42 MAPK/Erk2 (4, 5)]. Full activation of MAPKK also requires phosphorylation of two sites [Ser-218 and Ser-222 in mouse Mek-1/MKK1 (6–10)]. Detailed mechanisms for the activation of various MAPKKKs (e.g., Raf-1, B-Raf, Mos) are not yet established; here we assume that MAPKKKs are activated and inactivated by enzymes we denote E1 and E2. MAPKKK* denotes activated MAPKKK. MAPKK-P and MAPKK-PP denote singly and doubly phosphorylated MAPKK, respectively. MAPK-P and MAPK-PP denote singly and doubly phosphorylated MAPK. P'ase denotes phosphatase.

ultrasensitive enzymes are also relatively *less* sensitive to small stimuli than are Michaelis–Menten enzymes; at low stimulus levels their stimulus/response curves are less steep than those of Michaelis–Menten enzymes (Fig. 2*A*). Thus, highly ultrasensitive enzymes tend toward all-or-none, switch-like responses.

The most widely appreciated mechanism for generating ultrasensitive responses is cooperativity. Positively cooperative enzymes have sigmoidal stimulus/response curves, and require less than an 81-fold stimulus to drive them from 10% to 90% maximal response. However, cooperativity is not the only mechanism through which ultrasensitive responses can be generated. Ultrasensitivity also arises when enzyme cycles operate near saturation ["zero-order ultrasensitivity" (11)] and when stimuli impinge upon multiple steps of an enzyme cascade ["multistep ultrasensitivity" (12–14)].

We have investigated whether an ultrasensitive, switch-like response would be expected of the vertebrate Erk1/Erk2 MAPK cascade, given what is known about the abundances of the members of the cascade and their affinities for each other. We solved the rate equations for the cascade numerically, and found that the dose/response curves for MAPK and MAPKK are predicted to be sigmoidal, with the MAPK curve predicted to be as steep as that of a cooperative enzyme with a Hill coefficient of nearly 5. We then carried out detailed measurements of the stimulus/response curves for one MAPKK (Mek-1) and one MAPK (p42 MAPK/Erk2) in a highly

The publication costs of this article were defrayed in part by page charge payment. This article must therefore be hereby marked "*advertisement*" in accordance with 18 U.S.C. §1734 solely to indicate this fact.

Abbreviations: MAPK, mitogen-activated protein kinase; MAPKK, MAPK kinase; MAPKKK, MAPK kinase kinase.

†To whom reprint requests should be addressed.

manipulable system, *Xenopus* oocyte extracts. We found that p42 MAPK does exhibit a steep sigmoidal stimulus/response curve, as predicted. Thus, the MAPK cascade can convert a graded input into a switch-like output.

MATERIALS AND METHODS

Calculations. Eqs. **1-10** represent the reactions of the MAPK cascade, which are shown schematically in Fig. 1. We have used Goldbeter and Koshland's nomenclature for the rate constants—the letter a denotes association, d denotes dissociation without catalysis, and k denotes product formation (11). KKK denotes MAPKKK; KK denotes MAPKK; and K denotes MAPK.

$$\mathrm{KKK} + \mathrm{E1} \underset{d_1}{\overset{a_1}{\rightleftarrows}} \mathrm{KKK{\cdot}E1} \xrightarrow{k_1} \mathrm{KKK^*} + \mathrm{E1} \quad [1]$$

$$\mathrm{KKK^*} + \mathrm{E2} \underset{d_2}{\overset{a_2}{\rightleftarrows}} \mathrm{KKK{\cdot}E2} \xrightarrow{k_2} \mathrm{KKK} + \mathrm{E2} \quad [2]$$

$$\mathrm{KK} + \mathrm{KKK^*} \underset{d_3}{\overset{a_3}{\rightleftarrows}} \mathrm{KK{\cdot}KKK^*} \xrightarrow{k_3} \mathrm{KK\text{-}P} + \mathrm{KKK^*} \quad [3]$$

$$\mathrm{KK\text{-}P} + \mathrm{KK\ P'ase} \underset{d_4}{\overset{a_4}{\rightleftarrows}} \mathrm{KK\text{-}P{\cdot}KK\ P'ase} \xrightarrow{k_4} \mathrm{KK} + \mathrm{KK\ P'ase} \quad [4]$$

$$\mathrm{KK\text{-}P} + \mathrm{KKK^*} \underset{d_5}{\overset{a_5}{\rightleftarrows}} \mathrm{KK\text{-}P{\cdot}KKK^*} \xrightarrow{k_5} \mathrm{KK\text{-}PP} + \mathrm{KKK^*} \quad [5]$$

$$\mathrm{KK\text{-}PP} + \mathrm{KK\ P'ase} \underset{d_6}{\overset{a_6}{\rightleftarrows}} \mathrm{KK\text{-}PP{\cdot}KK\ P'ase} \xrightarrow{k_6} \mathrm{KK\text{-}P} + \mathrm{KK\ P'ase} \quad [6]$$

$$\mathrm{KK\text{-}PP} + \mathrm{K} \underset{d_7}{\overset{a_7}{\rightleftarrows}} \mathrm{KK\text{-}PP{\cdot}K} \xrightarrow{k_7} \mathrm{KK\text{-}PP} + \mathrm{K\text{-}P} \quad [7]$$

$$\mathrm{K\text{-}P} + \mathrm{K\ P'ase} \underset{d_8}{\overset{a_8}{\rightleftarrows}} \mathrm{K\text{-}P{\cdot}K\ P'ase} \xrightarrow{k_8} \mathrm{K} + \mathrm{K\ P'ase} \quad [8]$$

$$\mathrm{K\text{-}P} + \mathrm{KK\text{-}PP} \underset{d_9}{\overset{a_9}{\rightleftarrows}} \mathrm{K\text{-}P{\cdot}KK\text{-}PP} \xrightarrow{k_9} \mathrm{K\text{-}PP} + \mathrm{KK\text{-}PP} \quad [9]$$

$$\mathrm{K\text{-}PP} + \mathrm{K\ P'ase} \underset{d_{10}}{\overset{a_{10}}{\rightleftarrows}} \mathrm{KK\text{-}PP{\cdot}K\ P'ase} \xrightarrow{k_{10}} \mathrm{K\text{-}P} + \mathrm{K\ P'ase} \quad [10]$$

We assumed that other reactants (Mg^{2+} ATP, water) are present at constant concentration and so can be included in the rate constants.

The 10 reactions described above give rise to 18 rate equations.

$$\frac{d}{dt}[\mathrm{KKK}] = -a_1[\mathrm{KKK}][\mathrm{E1}] + d_1[\mathrm{KKK{\cdot}E1}] + k_2[KKK^* \cdot E2] \quad [11]$$

$$\frac{d}{dt}[\mathrm{KKK{\cdot}E1}] = a_1[\mathrm{KKK}][\mathrm{E1}] - (d_1 + k_1)[\mathrm{KKK{\cdot}E1}] \quad [12]$$

$$\frac{d}{dt}[\mathrm{KKK^*}] = -a_2[\mathrm{KKK^*}][\mathrm{E2}] + d_2[\mathrm{KKK^*{\cdot}E2}] + k_1[KKK \cdot E1] + (k_3 + d_3)[KK \cdot KKK^*] - a_3[KKK^*][KK] + (k_5 + d_5)[KK\text{-}P \cdot KKK^*] - a_5[KK\text{-}P][KKK^*] \quad [13]$$

$$\frac{d}{dt}[\mathrm{KKK^*{\cdot}E2}] = a_2[\mathrm{KKK^*}][\mathrm{E2}] - (d_2 + k_2)[\mathrm{KKK^*{\cdot}E2}] \quad [14]$$

$$\frac{d}{dt}[\mathrm{KK}] = -a_3[\mathrm{KK}][\mathrm{KKK^*}] + d_3[\mathrm{KK{\cdot}KKK^*}] + k_4[KK\text{-}P \cdot KK\ P'ase] \quad [15]$$

$$\frac{d}{dt}[\mathrm{KK{\cdot}KKK^*}] = a_3[\mathrm{KK}][\mathrm{KKK^*}] - (d_3 + k_3)[KK \cdot KKK^*] \quad [16]$$

$$\frac{d}{dt}[\mathrm{KK\text{-}P}] = -a_4[\mathrm{KK\text{-}P}][\mathrm{KK\ P'ase}] + d_4[\mathrm{KK\text{-}P{\cdot}KK\ P'ase}] + k_3[KK \cdot KKK^*] + k_6[KK\text{-}PP \cdot KK\ P'ase] + d_5[KK\text{-}P \cdot KKK^*] - a_5[KK\text{-}P][KKK^*] \quad [17]$$

$$\frac{d}{dt}[\mathrm{KK\text{-}P{\cdot}KK\ P'ase}] = a_4[\mathrm{KK\text{-}P}][\mathrm{KK\ P'ase}] - (d_4 + k_4)[KK\text{-}P \cdot KK\ P'ase] \quad [18]$$

$$\frac{d}{dt}[\mathrm{KK\text{-}P{\cdot}KKK^*}] = a_5[\mathrm{KK\text{-}P}][\mathrm{KKK^*}] - (d_5 + k_5)[KK\text{-}P \cdot KKK^*] \quad [19]$$

$$\frac{d}{dt}[\mathrm{KK\text{-}PP}] = k_5[\mathrm{KK\text{-}P{\cdot}KKK^*}] - a_6[\mathrm{KK\text{-}PP}][\mathrm{KK\ P'ase}] + d_6[KK\text{-}PP \cdot KK\ P'ase] - a_7[KK\text{-}PP][K] + (d_7 + k_7)[K \cdot KK\text{-}PP] + (d_9 + k_9)[K\text{-}P \cdot KK\text{-}PP] - a_9[K\text{-}P][KK\text{-}PP] \quad [20]$$

$$\frac{d}{dt}[\mathrm{KK\text{-}PP{\cdot}KK\ P'ase}] = a_6[\mathrm{KK\text{-}PP}][\mathrm{KK\ P'ase}] - (d_6 + K_6)[\mathrm{KK\text{-}PP{\cdot}KK\ P'ase}] \quad [21]$$

$$\frac{d}{dt}[\mathrm{K}] = -a_7[\mathrm{K}][\mathrm{KK\text{-}PP}] + d_7[\mathrm{K{\cdot}KK\text{-}PP}] + k_8[K\text{-}P \cdot K\ P'ase] \quad [22]$$

$$\frac{d}{dt}[\mathrm{K{\cdot}KK\text{-}PP}] = a_7[\mathrm{K}][\mathrm{KK\text{-}PP}] - (d_7 + k_7)[\mathrm{K{\cdot}KK\text{-}PP}] \quad [23]$$

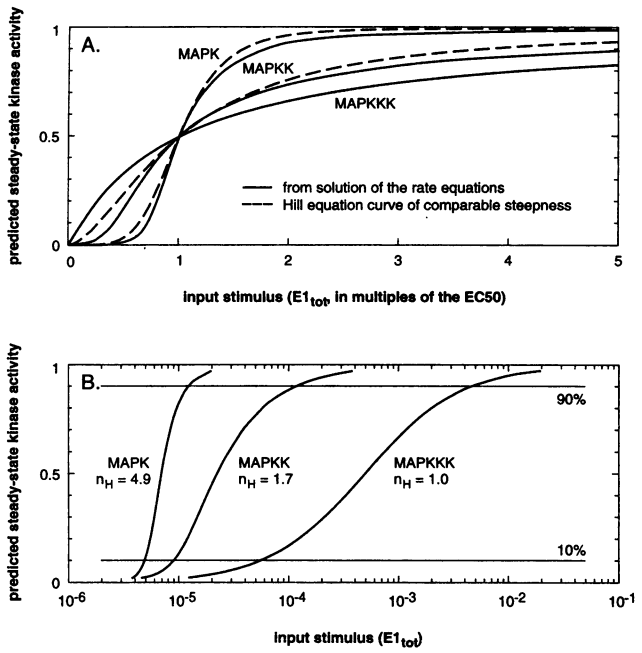

FIG. 2. Predicted stimulus/response curves for MAPK cascade components calculated by numerical solution of the rate equations for the MAP kinase cascade. (*A*) Predicted responses (solid lines) on a linear plot. The input stimulus is expressed in multiples of the EC_{50}, the concentration of $E1_{tot}$ that produces a 50% maximal response. The dashed lines are Hill equation curves whose steepness (the ratio of their EC_{90} to EC_{10}) is the same as the steepness of the calculated curves. (*B*) A semi-logarithmic plot of the predicted responses. Here the input stimulus ($E1_{tot}$) is expressed in absolute, rather than relative, terms.

$$\frac{d}{dt}[\text{K-P}] = k_7[\text{K·KK-PP}] - a_8[\text{K-P}][\text{K P'ase}] + d_8[K\text{-}P \cdot K\,P'ase] - a_9[K\text{-}P][KK\text{-}PP] + d_9[K\text{-}P \cdot KK\text{-}PP] + k_{10}[K\text{-}PP \cdot K\,P'ase] \quad [24]$$

$$\frac{d}{dt}[\text{K-P·K P'ase}] = a_8[\text{K-P}][\text{K P'ase}] - (d_8 + k_8)[K\text{-}P \cdot K\,P'ase] \quad [25]$$

$$\frac{d}{dt}[\text{K-P·KK-PP}] = a_9[\text{K-P}][\text{KK-PP}] - (d_9 + k_9)[K\text{-}P \cdot KK\text{-}PP] \quad [26]$$

$$\frac{d}{dt}[\text{K-PP}] = -a_{10}[\text{K-PP}][\text{K P'ase}] + d_{10}[K\text{-}PP \cdot K\,P'ase] + k_9[K\text{-}P \cdot KK\text{-}PP] \quad [27]$$

$$\frac{d}{dt}[\text{K-PP·K P'ase}] = a_{10}[\text{K-PP}][\text{K P'ase}] - (d_{10} + k_{10})[K\text{-}PP \cdot K\,P'ase] \quad [28]$$

In addition, there are seven conservation equations (Eqs. **29-35**).

$$[\text{KKK}_{tot}] = [\text{KKK}] + [\text{KKK*}] + [\text{KKK·E1}] + [KKK^* \cdot E2] + [KKK^* \cdot K] + [KKK^* \cdot K\text{-}P] \quad [29]$$

$$[\text{E1}_{tot}] = [\text{E1}] + [\text{KKK·E1}] \quad [30]$$

$$[\text{E2}_{tot}] = [\text{E2}] + [\text{KKK*·E2}] \quad [31]$$

$$[\text{KK}_{tot}] = [\text{KK}] + [\text{KK-P}] + [\text{KK-PP}] + [\text{KK·KKK*}] + [KK\text{-}P \cdot KKK^*] + [KK\text{-}P \cdot KK\,P'ase] + [KK\text{-}PP \cdot KK\,P'ase] + [KK\text{-}PP \cdot K] + [KK\text{-}PP \cdot K\text{-}P] \quad [32]$$

$$[\text{KK P'ase}_{tot}] = [\text{KK P'ase}] + [\text{KK P'ase·KK-P}] + [KK\,P'ase \cdot KK\text{-}PP] \quad [33]$$

$$[\text{K}_{tot}] = [\text{K}] + [\text{K-P}] + [\text{K-PP}] + [\text{KK-PP·K}] + KK\text{-}PP \cdot K\text{-}P] + [K\text{-}P \cdot K\,P'ase] + [K\text{-}PP \cdot K\,P'ase] \quad [34]$$

$$[\text{K P'ase}_{tot}] = [\text{K P'ase}] + [\text{K-P·K P'ase}] + [K\text{-}PP \cdot K\,P'ase] \quad [35]$$

These equations were solved numerically using the Runge–Kutta-based NDSolve algorithm in Mathematica (Wolfram Research, Champaign, IL). An annotated copy of the Mathematica code for the MAPK cascade rate equations can be obtained from J.E.F.

The equations written above assume that the dual phosphorylations of MAPK and MAPKK occur by two-step, distributive mechanisms. MAPK collides with its activator (MAPKK-PP), undergoes the first phosphorylation, and is released by its activator; then the monophosphorylated MAPK-P collides with MAPKK-PP, undergoes the second phosphorylation, and is released as active MAPK-PP (and likewise for the double phosphorylation of MAPKK by MAPKKK*). We also set up and solved the equations for cascades where MAPK is activated in a two-step process but MAPKK is activated by a one-collision, processive mechanism; where MAPK is activated by a one-collision mechanism but MAPKK is activated by a two-collision mechanism; or where both enzymes are activated by one-collision, processive mechanisms, as described below.

Assumed Concentrations and K_m Values. We initially assumed the total concentrations of MAPKKK, MAPKK, and MAPK to be 3 nM, 1.2 μM, and 1.2 μM, respectively, based on estimates for the concentrations of Mos (a MAPKKK), Mek-1 (a MAPKK), and p42 MAPK, in mature *Xenopus* oocytes (17–19). We initially assumed that $E2_{tot}$ is 0.3 nM (10-fold less abundant than its substrate Mos); that MAPKK $P'ase_{tot}$ is 0.3 nM (so that the maximal concentration of activated MAPKKK is 10-fold higher than that of this opposing phosphatase); and that MAPK $P'ase_{tot}$ is 120 nM (so that the maximal concentration of activated MAPKK is 10-fold higher than that of this opposing phosphatase). $E1_{tot}$ was taken to represent the level of input stimulus to the cascade, and was varied over a wide range.

For the purposes of calculating steady-state levels of the enzyme species, it is the K_m values [$K_{mx} = (d_x + k_x)/a_x$] rather than the individual rate constants that are pertinent. We initially assumed the K_m value for phosphorylation of MAPK by MAPKK-PP to be 300 nM, based on a value measured for the phosphorylation of mammalian p42 MAPK/Erk2 by active MKK-1 (N. Ahn, personal communication), and arbitrarily took all of the other K_m values to be 300 nM as well. We subsequently varied all of these K_m values and concentrations over a 25-fold range.

In the numerical studies, the input stimulus to the cascade was taken to be the concentration of $E1_{tot}$, whereas in the experimental studies, what was varied was the concentration of Mos_{tot} (the relevant MAPKKK). However, the calculated

curves for MAPK or MAPKK activation versus [$MAPKKK_{tot}$] are similar in steepness to those for MAPK or MAPKK activation versus [$E1_{tot}$]. For example, if [$E1_{tot}$] is fixed at 0.01 nM and [Mos_{tot}] is varied, the predicted Hill coefficients for MAPK and MAPKK are 5.0 and 1.7, respectively.

Experimental Studies. Concentrated *Xenopus* oocyte extracts were prepared as described (20–22). Briefly, oocytes were defolliculated, washed twice with extract buffer (0.25 M sucrose/0.1 M NaCl/2.5 mM $MgCl_2$/20 mM Hepes, pH 7.2/10 μg leupeptin per ml/10 μg pepstatin per ml/10 μg chymostatin per ml/10 μg aprotinin per ml/1 mM phenylmethylsulfonyl flouride), and twice with extract buffer supplemented with 100 μg cytochalasin B per ml. The washed, defolliculated oocytes were centrifuged at low speeds to remove excess buffer, and crushed by centrifugation. The cytoplasm was collected, clarified by centrifugation, and stored at −80°C.

Thawed extracts (7 volumes) were mixed with an ATP regenerating system (20 mM ATP/20 mM $MgCl_2$/200 mM creatine phosphate/1 mg creatine kinase per ml; 1 volume); various concentrations of bacterially-expressed malE-Mos (18) (2 volumes in extract buffer) were added, and the reactions were incubated at room temperature for 100 min. This length of time was sufficient to allow Mek-1 and p42 MAPK to reach steady-state activity levels (data not shown).

The steady-state activity of Mek-1 was assessed by a linked immune complex kinase assay, and the activity of p42 MAPK by a myelin basic protein kinase assay (23). Care was taken to ensure that the Mek-1 and p42 MAPK activity assays were linear with respect to time and enzyme concentration (data not shown). The phosphorylation state of p42 MAPK was also assessed by immunoblotting; phosphorylated forms of p42 MAPK exhibit a retarded electrophoretic mobility (24).

RESULTS

Predicted Stimulus/Response Relationships. We set up and numerically solved the rate equations for the reactions shown in Fig. 1. We assumed that the MAPK and MAPKK phosphorylation reactions occurred in two steps, as indicated in Fig. 1, and that neither step was markedly more rapid than the other. We initially fixed the enzyme concentrations and K_m values that have been measured for vertebrate Erk/MAPK cascade components and assumed reasonable values for the unknown concentrations and K_m values.

As shown in Fig. 2, the stimulus/response curve predicted for MAPKKK is that of a typical Michaelis–Menten enzyme. It is hyperbolic on a linear plot (Fig. 2*A*) and sigmoidal on a semi-logarithmic plot (Fig. 2*B*). An 81-fold increase in stimulus is needed to drive the MAPKKK response from 10% maximal to 90% maximal. In contrast, the stimulus/response curves predicted for MAPKK and MAPK are sigmoidal on linear plots (Fig. 2*A*) and steeply sigmoidal on semi-logarithmic plots (Fig. 2*B*). The predicted curves are similar in shape to those given by the Hill equation ($y = x^{nH}/[K + x^{nH}]$), but are steeper at low stimulus levels and less steep at high stimulus levels (Fig. 2*A*). A 13-fold increase in stimulus is predicted to drive MAPKK from 10% maximal activation to 90%, and the number falls to 2.5-fold for MAPK. Using the expression $n_H = \log(EC_{90}/EC_{10})/\log 81$ for the Hill coefficient of a cooperative protein (25), the responses of MAPKK and MAPK are calculated to be equivalent to those of cooperative enzymes with Hill coefficients of 1.7 and 4.9, respectively. The Hill coefficient predicted for the MAPK response exceeds that of the canonical cooperative protein hemoglobin, whose Hill coefficient for oxygen binding is 2.8 (26).

Because many of the K_m values and concentrations were assumed rather than measured, it was important to determine whether ultrasensitivity would be predicted for a range of other values. We varied the assumed concentrations (Table 1) and K_m values (Table 2) for all of the cascade enzymes and reactions 25-fold, and calculated Hill coefficients for the MAPK, MAPKK, and MAPKKK responses. MAPKKK was invariably predicted to respond like a normal Michaelis–Menten enzyme with a Hill coefficient of 1. MAPKK was predicted to exhibit an ultrasensitive response, with its Hill coefficient ranging from 1.3 to 2.4 (Tables 1 and 2). MAPK was invariably predicted to be more highly ultrasensitive than MAPKK, with its Hill coefficient ranging from 2.4 to 9.1 (Tables 1 and 2). Thus, the prediction that MAPK and MAPKK exhibit ultrasensitive responses is robust, although the exact degree of ultrasensitivity predicted varies with the assumed concentrations and K_m values.

Contributions from Zero-Order Ultrasensitivity. As shown in Table 1, the predicted ultrasensitivity of MAPK depended upon the assumed concentration of MAPKK more sensitively than it did upon the assumed concentrations of the other cascade enzymes. If the concentration of MAPKK was assumed to be 6 μM [5-fold greater than the concentration initially assumed and 20-fold above the measured K_m value for the phosphorylation of MAPK by active MAPKK (300 nM)], the Hill coefficient predicted for MAPK would be 9.1 (Table 1). Similarly, if all of the reactions in which MAPKK participates (Eqs. **3-7** and **9**) had K_m values of 60 nM rather than the initially-assumed 300 nM, the predicted Hill coefficient for MAPK would be 8.5 (not shown); if only the reactions that convert MAPKK among its various phosphorylation states had K_m values of 60 nM (Eqs. **3-6**), the predicted Hill coefficient for MAPK would be 9.4 (not shown). Thus, the concentration of MAPKK relative to the K_m values for the reactions that activate and inactivate is important in determining the MAPK

Table 1. Predicted Hill coefficients for MAPK cascade components: Varying the assumed enzyme concentrations

Enzyme	Range of assumed concentrations	Range of effective Hill coefficients (nH) predicted for		
		MAPKKK	MAPKK	MAPK
MAPKKK	0.6–15 nM (3 nM†)	0.9–1.0	1.6–1.7	3.8–5.1
MAPKK	0.24–6 μM (1.2 μM†)	1.0	1.4–1.9	2.4–9.1
MAPK	0.24–6 μM (1.2 μM†)	1.0	1.7	3.8–5.1
E2 (MAPKKK inactivase)	0.06–1.5 nM	1.0	1.7	4.9
MAPKK P′ase	0.06–1.5 nM	1.0–1.1	1.6–1.7	3.8–5.1
MAPK P′ase	24–600 nM	1.0	1.6–1.7	2.5–5.1

The assumed concentrations of each enzyme were individually varied over the ranges shown, with the assumed concentrations of the other five enzymes held constant. The effective Hill coefficients were calculated from the steepness of the predicted stimulus/response curves, as described in the text.

†The numbers shown in parentheses are estimated values for the concentrations of Mos (a MAPKKK), Mek-1 (a MAPKK), and p42 MAPK (a MAPK) in *Xenopus* oocytes. We initially assumed [E2] to be 0.3 nM, [MAPKK P′ase] to be 0.3 nM, and [MAPK P′ase] to be 120 nM. See text for details.

Table 2. Predicted Hill coefficients for MAP kinase cascade components: Varying the assumed K_m values

Reaction	Range of assumed K_m values	Range of effective Hill coefficients (nH) predicted for MAPKKK	MAPKK	MAPK
1. MAPKKK → MAPKKK*	60–1500 nM	1.0	1.7	4.9
2. MAPKKK* → MAPKKK	60–1500 nM	1.0	1.7	4.9
3. MAPKK → MAPKK-P	60–1500 nM	1.0	1.3–2.3	4.0–5.1
4. MAPKK-P → MAPKK	60–1500 nM	1.0	1.5–1.9	3.6–6.7
5. MAPKK-P → MAPKK-PP	60–1500 nM	1.0	1.3–2.4	3.8–5.2
6. MAPKK-PP → MAPKK-P	60–1500 nM	1.0	1.7–1.8	4.1–6.4
7. MAPK → MAPK-P	60–1500 nM (300 nM†)	1.0	1.7	3.7–6.2
8. MAPK-P → MAPK	60–1500 nM	1.0	1.7	4.3–5.2
9. MAPK-P → MAPK-PP	60–1500 nM	1.0	1.7	3.4–6.1
10. MAPK-PP → MAPK-P	60–1500 nM	1.0	1.7	4.7–5.1

The assumed K_m values for each reaction were individually varied over the ranges shown, with the assumed K_m values for the other nine reactions held constant. The effective Hill coefficients were calculated from the steepness of the predicted stimulus/response curves, as described in the text.

†The K_m value for reaction 7 has been measured to be 300 nM for the phosphorylation of a mammalian MAPK by a MAPKK (N. Ahn, personal communication). All of the other K_m values were initially assumed to be 300 nM as well.

response; zero-order ultrasensitivity contributes to the overall response of the cascade.‡

The Role of Dual Phosphorylation. As shown in Table 3, the high degree of ultrasensitivity was found to depend critically upon the assumption that the dual phosphorylation of MAPKK and MAPK occurred by two-collision mechanisms. Assuming a single-collision, processive mechanism for phosphorylation of both kinases reduced the predicted Hill coefficient for MAPKK from 1.7 to 1.3 and reduced the predicted Hill coefficient for MAPK from 4.9 to 1.5. Both of the two-collision mechanisms were found to contribute to the steepness of the MAPK stimulus/response curve, whereas the steepness of the MAPKK stimulus/response curve depended only on the assumption that MAPKK was activated by a two-collision mechanism (Table 1). A single-collision mechanism for both MAPKK and MAPK activation would permit high degrees of ultrasensitivity only if the concentration of MAPKK present in cells were substantially higher than what has been measured for Mek-1.

The connection between a two-collision mechanism for kinase activation and a sigmoidal, ultrasensitive response can be rationalized by considering the expected stimulus/response curves for the first and the second phosphorylation of one of the enzymes (e.g., MAPKK) for the special case of a small input stimulus. The first phosphorylation is driven by a linearly increasing input stimulus (MAPKKK*) and a constant concentration of its substrate (MAPKK). The result is that the rate and equilibrium level of phosphorylation of the substrate increase linearly with the input stimulus. The second phosphorylation is driven by a linearly increasing input stimulus (MAPKKK*) and a linearly increasing substrate concentration (singly phosphorylated MAPKK), so the rate and equilibrium of the second phosphorylation increase as the square of the input stimulus. Thus, the stimulus/response relationship initially curves upward. The response must approach a limit as the stimulus is increased to high levels, and the overall result is a sigmoidal stimulus/response relationship.

Summary of Calculations. The MAPK cascade is predicted to exhibit ultrasensitivity, with the degree of ultrasensitivity increasing as the cascade is descended. This behavior is robustly predicted for a wide range of assumed concentrations and K_m values for the cascade enzymes and reactions, although the exact extent of the predicted ultrasensitivity varies as the assumed values are varied.

Experimental Studies of MAPK and MAPKK Activation in *Xenopus* Oocyte Extracts. We chose to test the predicted ultrasensitivity in a highly manipulable experimental system, *Xenopus* oocyte extracts (20, 28, 29). These extracts possess a MAPK (p42 MAPK/Erk2), a MAPKK (Mek-1/MKK-1), and Mos activating enzymes, but no Mos (the relevant MAPKKK). We added various concentrations of recombinant malE-Mos to the extracts and monitored the responses of Mek-1 and p42 MAPK.

‡Bardwell and colleagues have recently estimated the abundance of two budding yeast MAPK, Kss1p and Fus3p, to be roughly 5000 molecules per cell, and the abundance of the MAPKK Ste7p to be fewer than 2000 molecules per cell (27). Assuming a cytoplasmic volume of 0.1 pL for a haploid yeast, these abundances correspond to concentrations of 100 and <35 nM, respectively, substantially lower than the concentrations measured in *Xenopus* oocytes and mammalian tissue culture cells and assumed here in our calculations (1.2 μM). However, the affinity of the yeast kinases for each other also appears to be higher than those of their vertebrate counterparts. Kss1p and Ste7p associate with an affinity of about 5 nM (27), as opposed to a K_m value of 300 nM for the phosphorylation of rodent MAPK by active MAPKK (N. Ahn, personal communication). So, in both cases, the enzyme (MAPKK) and its substrate (MAPK) are present at concentrations that are high relative to their affinities (K_d values or K_m values) for each other. Possibly these higher affinity interactions allow the yeast enzymes to produce switch-like responses with lower concentrations of the cascade enzymes.

Table 3. Predicted Hill coefficients for MAPK cascade components assuming one-step (processive) or two-step (distributive) models for the phosphorylation of MAPK and MAPKK

Model	Effective Hill coefficient (nH) predicted for: MAPKKK	MAPKK	MAPK
One-step phosphorylation for MAPKK activation; One-step phosphorylation for MAPK activation	1.0	1.3	1.5
One-step phosphorylation for MAPKK activation; Two-step phosphorylation for MAPK activation	1.0	1.3	2.0
Two-step phosphorylation for MAPKK activation; One-step phosphorylation for MAPK activation	1.0	1.7	3.7
Two-step phosphorylation for MAPKK activation; Two-step phosphorylation for MAPK activation	1.0	1.7	4.9

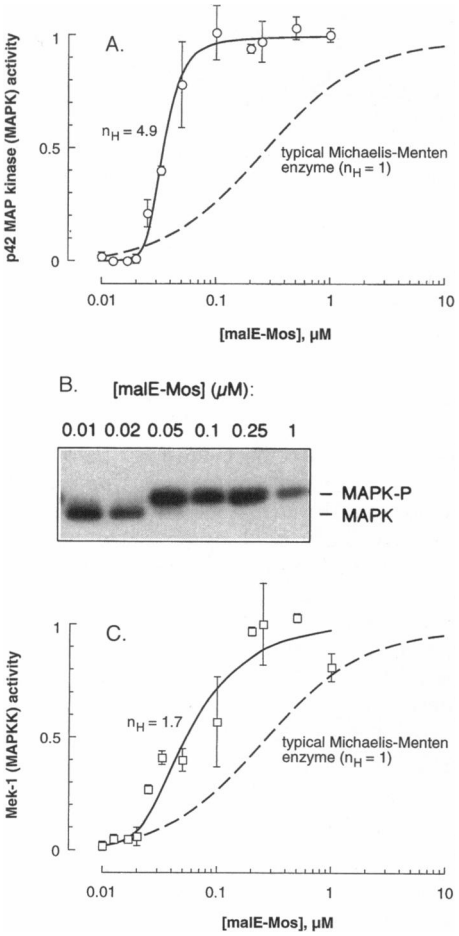

FIG. 3. Experimental stimulus/response data for MAPK and MAPKK activation. *Xenopus* oocyte extracts were treated with various concentrations of purified, bacterially expressed malE-Mos, and MAPK and MAPKK activities were assessed after the kinases reached steady state. The activity data shown in *A* (p42 MAPK activation, ○) and *C* (Mek-1 activation, □) are pooled from two independent experiments. Error bars represent 1 SD; $n = 4$ for six of the malE-Mos concentrations (0.01, 0.02, 0.05, 0.1, 0.5, and 1 μM) and $n = 2$ for the other six (0.013, 0.017, 0.025, 0.033, 0.2, and 0.25 μM). The MAPK blot shown in *B* was taken from a single experiment. The upper band represents phosphorylated p42 MAPK, and the lower band nonphosphorylated p42 MAPK. The kinase-minus K52R mutant form of malE-Mos brought about no activation or phosphorylation of either MAPK or MAPKK (data not shown).

As shown in Fig. 3 *A* and *B*, the activation of p42 MAPK was found to be a steep sigmoidal function of the amount of malE-Mos added to the extract, as predicted. The steepness of the response was evident both from the myelin basic protein kinase assay data (Fig. 3*A*) and from the mobility shift data (Fig. 3*B*). Mek-1 activation was found to be a less steeply sigmoidal function of the amount of malE-Mos added to the extract (Fig. 3*C*). The experimental data are in excellent agreement with the predicted nH = 4.9 (p42 MAPK) and nH = 1.7 (Mek-1) curves (Fig. 3 *A* and *C*). The amount of malE-Mos needed to half-maximally activate p42 MAPK was lower than the amount needed to half-maximally activate Mek-1 (Fig. 3 *A* and *C*), again as predicted.

DISCUSSION

Here we have demonstrated that the MAPK cascade converts graded inputs into switch-like outputs. The stimulus/response curves of the enzymes can be accounted for by the known reactions of the MAPK cascade, if it is assumed that MAPK and MAPKK are activated by two-collision mechanisms and that the reactions that activate and inactivate MAPKK are partially saturated. Clearly it will be of interest to test the validity of these assumptions, to determine whether the scheme shown in Fig. 1 is incomplete in some important way.

We suspect that ultrasensitivity is important for the biological function of the MAPK cascade. The cascade should be able to filter out noise—respond less to small stimuli than a single Michaelis–Menten enzyme would—and then flip from off to on over a narrow range of input stimuli. This sort of behavior would be particularly appropriate for a signaling system that mediates processes like mitogenesis, cell fate induction, and oocyte maturation, where cells switch rapidly between discrete states without assuming stable intermediate positions.

Note Added in Proof. We have recently determined that MAPK is phosphorylated by MAPKK through a two-collision, distributive mechanism *in vitro*, and that the MAP kinase phosphatase activity in an oocyte extract is partially saturated under physiological conditions (apparent $K_m \approx 300$ nM). These findings validate key assumptions that underpinned the prediction of a highly ultrasensitive response for MAPK.

We thank B. Osgood and R. Pattis for aiming us toward Mathematica; G. Vande Woude for providing malE-Mos plasmids; M. Cobb, J. Cooper, T. Geppert, and J. Posada for providing MAPK plasmids; N. Ahn and J. Thorner for communicating unpublished results; and members of the Ferrell laboratory for helpful comments on this manuscript. This work was supported by National Institutes of Health Grant GM46383 and by a Faculty Development Award from the Pharmaceutical Research and Manufacturers of America Foundation.

1. Marshall, C. J. (1994) *Curr. Opin. Genet. Dev.* **4,** 82–89.
2. Cobb, M. H. & Goldsmith, E. J. (1995) *J. Biol. Chem.* **270,** 14843–14846.
3. Ferrell, J. E., Jr. (1996) *Curr. Top. Dev. Biol.* **33,** 1–60.
4. Anderson, N. G., Maller, J. L., Tonks, N. K. & Sturgill, T. W. (1990) *Nature (London)* **343,** 651–653.
5. Payne, D. M., Rossomando, A. J., Martino, P., Erickson, A. K., Her, J.-H., Shabanowitz, J., Hunt, D. F., Weber, M. J. & Sturgill, T. W. (1991) *EMBO J.* **10,** 885–892.
6. Resing, K. A., Mansour, S. J., Hermann, A. S., Johnson, R. S., Candia, J. M., Fukasawa, K., Vande Woude, G. F. & Ahn, N. G. (1995) *Biochemistry* **34,** 2610–2620.
7. Alessi, D. R., Saito, Y., Campbell, D. G., Cohen, P., Sithanandam, G., Rapp, U., Ashworth, A., Marshall, C. J. & Cowley, S. (1994) *EMBO J.* **13,** 1610–1619.
8. Zheng, C. F. & Guan, K. L. (1994) *EMBO J.* **13,** 1123–1131.
9. Huang, W. & Erikson, R. L. (1994) *Proc. Natl. Acad. Sci. USA* **91,** 8960–8963.
10. Pages, G., Brunet, A., L'Allemain, G. & Pouyssegur, J. (1994) *EMBO J.* **13,** 3003–3010.
11. Goldbeter, A. & Koshland, D. E., Jr. (1981) *Proc. Natl. Acad. Sci. USA* **78,** 6840–6844.
12. Koshland, D. E., Jr., Goldbeter, A. & Stock, J. B. (1982) *Science* **217,** 220–225.
13. Goldbeter, A. & Koshland, D. E., Jr. (1982) *Q. Rev. Biophys.* **15,** 555–591.
14. Goldbeter, A. & Koshland, D. E., Jr. (1984) *J. Biol. Chem.* **259,** 14441–14447.
15. Chock, P. B. & Stadtman, E. R. (1977) *Proc. Natl. Acad. Sci. USA* **74,** 2766–2770.
16. Chock, P. B., Rhee, S. G. & Stadtman, E. R. (1980) *Annu. Rev. Biochem.* **49,** 813–843.
17. Matsuda, S., Kosako, H., Takenaka, K., Moriyama, K., Sakai, H., Akiyama, T., Gotoh, Y. & Nishida, E. (1992) *EMBO J.* **11,** 973–982.
18. Yew, N., Mellini, M. L. & Vande Woude, G. F. (1992) *Nature (London)* **355,** 649–652.
19. Haccard, O., Sarcevic, B., Lewellyn, A., Hartley, R., Roy, L., Izumi, T., Erikson, E. & Maller, J. L. (1993) *Science* **262,** 1262–1265.
20. Shibuya, E. K. & Ruderman, J. V. (1993) *Mol. Biol. Cell* **4,** 781–790.
21. Shibuya, E. K., Polverino, A. J., Chang, E., Wigler, M. & Ruderman, J. V. (1992) *Proc. Natl. Acad. Sci. USA* **89,** 9831–9835.
22. Nebreda, A. R., Hill, C., Gomez, N., Cohen, P. & Hunt, T. (1993) *FEBS Lett.* **333,** 183–187.
23. Huang, C.-Y. F. & Ferrell, J. E., Jr. (1996) *EMBO J.* **15,** 2169–2173.
24. Posada, J. & Cooper, J. A. (1992) *Science* **255,** 212–215.
25. Koshland, D. E., Jr., Nemethy, G. & Filmer, D. (1966) *Biochemistry* **5,** 365–385.
26. Stryer, L. (1988) *Biochemistry* (Freeman, New York).
27. Bardwell, L., Cook, J. G., Chang, E. C., Cairns, B. R. & Thorner, J. (1996) *Mol. Cell. Biol.* **16,** 3637–3650.
28. Nebreda, A. R. & Hunt, T. (1993) *EMBO J.* **12,** 1979–1986.
29. Posada, J., Yew, N., Ahn, N. G., Vande Woude, G. F. & Cooper, J. A. (1993) *Mol. Cell. Biol.* **13,** 2546–2553.